



A new method for linear feature and junction enhancement in 2D images based on morphological operation, oriented anisotropic Gaussian function and Hessian information

Ran Su ^{a,b,*}, Changming Sun ^b, Chao Zhang ^{a,b}, Tuan D. Pham ^c

^a School of Engineering and Information Technology, The University of New South Wales, Canberra, ACT 2600, Australia

^b CSIRO Computational Informatics, Locked Bag 17, North Ryde, NSW 1670, Australia

^c Aizu Research Cluster for Medical Engineering and Informatics, Research Center for Advanced Information Science and Technology, The University of Aizu, Aizu-Wakamatsu, Fukushima 965-8580, Japan

ARTICLE INFO

Article history:

Received 30 July 2013

Received in revised form

25 March 2014

Accepted 25 April 2014

Available online 9 May 2014

Keywords:

Linear feature

Enhancement

Morphological operation

Gaussian function

Hessian information

Junction

ABSTRACT

Feature enhancement is an important preprocessing step in many image processing tasks. It is the process of adjusting image intensities so that the enhanced results are more suitable for analysis. Good enhancement results for linear structures such as vessels or neurites can be used as inputs for segmentation and other operations. In this paper, a novel linear feature enhancement filter – an adaptive multi-scale morpho-Gaussian filter – which can enhance and smooth linear features is proposed based on morphological operation, anisotropic Gaussian function and Hessian information. This filter can enhance and smooth along the local orientation of the linear structures and the Hessian measurement is used to further enhance the linear features. We utilize the Hessian matrix to calculate the orientation information for our directional morphological operation and the oriented anisotropic Gaussian smoothing. We also propose a novel method for junction enhancement, which can solve the problem of junction suppression. We decompose the junctions and enhance along each linear structure within a junction region. We present the test results of our algorithm on images of different types and compare our method with three existing methods. The experimental results show that the proposed approach can achieve better results.

© 2014 Elsevier Ltd. All rights reserved.

1. Introduction

Many objects such as retinal vessels, neurites and plant roots have linear features. Information about these structures can be used in biomedical and other types of applications. By analyzing vessel structures, diseases that involve structural or functional changes can be investigated [1,2]. For example, hypertension may result in focal constriction of retinal arteries and arteriosclerosis can cause the arteries to show a copper or silver color [3,4]. Moreover, the number and morphology of neuron cells can be used to predict or diagnose brain diseases such as Alzheimer's disease, which is characterized by the loss of neurons and synapses in the cerebral cortex and certain subcortical regions [5]. Therefore, the detection, segmentation and tracking for linear

structures in images can release the biologists from heavy burden of manual work and improve efficiency.

However, the images that are to be segmented are not always of high quality due to distortions during acquisition, processing, compression, storage, transmission and reproduction, which will affect the result of segmentation or tracking [6]. The enhancement of linear features can make the image processing steps easier and greatly improve the result of feature segmentation. In medical image analysis, for example, enhancement of vessels can improve the visualization of vessels and small vessel delineation. It can also provide the input for vessel segmentation, centerline extraction and tracking.

In this paper, novel algorithms are proposed to enhance linear features as well as enhance junction regions without any suppression. Firstly, we propose an adaptive multi-scale morpho-Gaussian filter to enhance, reconnect and smooth linear features. From the Hessian matrix, the orientation of the features and a measurement based on the eigenvalues are obtained. At each pixel along its orientation, we carry out a linear morphological operation so that linear structures are enhanced and noisy structures are

* Corresponding author. Current address: Bioinformatics Institute, 30 Biopolis Street, #07-01 Matrix, Singapore 138671.

E-mail addresses: suran.tju@gmail.com (R. Su), changming.sun@csiro.au (C. Sun), kone.zhang@gmail.com (C. Zhang), tdpham@u-aizu.ac.jp (T.D. Pham).

suppressed. The intensity profile of the linear structure's cross section can be approximated by a Gaussian curve [7,8]. Multi-scale locally oriented anisotropic Gaussian templates are applied in each morphologically enhanced window to smooth the linear structures in our work. To match linear structures with various widths, the Gaussian function is used in multiple scales. The enhanced and reconnected features using the morphological operation are smoothed by using this multi-scale-anisotropic Gaussian function. Then a multi-scale Hessian-based filter is used to further enhance the linear structures. The enhancement results of existing methods in junction regions are not satisfactory because junctions are the intersection of several linear structures and have multiple orientations. To solve this issue, a novel method for junction enhancement is proposed. We first decompose the junctions into separate linear structures or branches, and then we enhance the linear features along each branch. In Section 2, we give a brief review of some of the existing approaches. Section 3 gives a brief overview about our algorithm. In Section 4, the linear feature enhancement approach is described. Our junction enhancement method is described in Section 5. We give experimental results and statistical analysis in Section 6. The paper is concluded in Section 7.

2. Related work

Due to the importance of linear feature enhancement, a variety of enhancement methods have been developed recently. Hessian based approach is one of the most popular methods, because the second order structure in the Hessian matrix describes the intensity variations for each point [9]. In Sato et al. and Lorenz et al.'s work, eigenvalues of the Hessian matrix were analyzed to determine the local likelihood of vesselness [10,11]. They constructed a line-structure-ness measure using the eigenvalues. Based on their work, Frangi et al. proposed another filter using a combination of the Hessian matrix eigenvalues to enhance vessel structures [12]. Their approach was able to preserve more details of the vessels than the previous methods. Lin improved Frangi et al.'s method to obtain a specialized detector, which was also based on the second order derivatives [13]. Orlowski and Orkisz used Hessian trace, determinant and sign to discard voxels unlikely to belong to vessels prior to the computation of the Hessian eigenvalues [14]. Shikata et al. proposed another combination of eigenvalues of the Hessian matrix to enhance vessel structures [15]. Different from Frangi et al.'s work, this method was able to enhance small vessels but not good at noise suppression. Olabarriaga et al. applied three Hessian-based enhancement methods: Lorenz et al. filter, Sato et al. filter and Frangi et al. filter and a comparison among the three methods was given in [16]. However, in the Hessian based methods, as the region where three or more vessels meet (known as the junction region) always has a similar response with that of blob-like structures, the junction region is always suppressed [17] or the enhancement for a junction region cannot achieve results as good as that for linear structures.

In recent years, several methods of enhancement of linear structures based on diffusion process have been proposed. In 1995, Deguchi et al. analyzed the resolution of images and used a structure tensor based diffusion process to enhance the images [18]. The diffusion direction was determined by the phase angle of the structure tensor. Another anisotropic diffusion scheme guided by a vesselness measure at each pixel was proposed by Cártero and Padeva [19]. In Krissian's work, a three dimensional basis based on minimal principal curvature direction of the isosurface was used to steer the diffusion [20]. But the gradient calculation along the vessel might cause a problem along the central axis since the gradient here was almost zero. Manniesing et al.'s method used a

Hessian eigen-system based diffusion tensor which satisfied a smoothness constraint and extended their method to 3D vessel images [21]. Based on Manniesing et al.'s method, Chen et al. developed a structure-preserving diffusion tensor which could achieve better performance [9]. Kroon et al. proposed an optimized scheme for the diffusion tensor, which was rotational invariant and showed good isotropic filtering behavior [22]. This type of methods was reported to have a good performance but they were extremely time-consuming.

Another type of approaches enhanced linear features based on morphological filters. Wilkinson and Westenberg used connected-set morphological filters to extract filamentous details considering their shape preserving property [23]. Tankyevych et al. proposed a method to enhance linear features along the orientation of each pixel in a structure element [24]. The orientation was calculated according to Frangi et al.'s filter [12]. This method was sensitive to noise and the enhancement in junction regions was not as good as that of linear features since multiple orientations were produced in junction regions where several linear structures met. Agam et al. proposed a method based on a correlation matrix [25]. In their study, eigenvalues of the correlation matrix were used to differentiate vessels, junctions and nodules. Then a filter was built based on this information. A method based on discrete curvelet transform was proposed by Miri and Mahloojifar [26]. The contrast between the linear features and the background was largely enhanced through their method. In Oh and Hwang's research, the image logarithm was decomposed into several subbands using morphological filters with various size of structure elements, then a homomorphic filtering was performed [27]. The morphological approaches sometimes could not effectively reduce the noise and sometimes would have the problem of junction suppression.

In our work, we propose a multi-scale morpho-Gaussian filter to enhance and smooth linear features. A morphological filter can be designed to suppress noise yet preserve geometrical structures in an image [28]. The earliest study can be traced back to 1960s [29–31]. An adaptive morphological operation was proposed to enhance the linear features and suppress noise. Matched filter with Gaussian kernel was used in many tasks for smoothing and enhancing purpose [7,32–36]. Inspired from their work, we use the oriented anisotropic Gaussian template in multiple scales to fit with linear structures with different widths. The Gaussian template is designed to convolve with the original image in order to enhance and smooth the linear structures. We combine the Hessian information, morphological operation with the oriented anisotropic Gaussian function and build a new filter so that linear structures can be enhanced and smoothed. The filter is conducted along the local orientation in each small window. Moreover, broken parts of linear features can be reconnected. Many visual tasks rely on junction extraction, because junction features provide very useful local information about the geometric properties and occlusions [37–39]. However, there is always a problem of junction suppression in existing Hessian based filters as there are multiple linear structures meeting at junctions. We propose a junction enhancement approach to solve this issue. A number of junction detection methods have been proposed as in [40–42]. Here we adopt the method described in [43] which can give an exact location of the junction center point and the orientations of the linear structures that meet at the junction. By using this junction detection method and linear feature enhancement along each branch, the problem of junction suppression can be solved. We also improve this junction detection method so that it can also be used in the detection of the ends of linear features. As described before, the Hessian-based filter provides a measurement of the likelihood of linear structures. A value based on Hessian matrix is used in the proposed morpho-Gaussian filter to measure the

magnitude of the linelikelihood. It can preserve more details than the Frangi et al.'s filter. Finally, another Hessian-based filter is used to further enhance the linear features.

3. Overview of the proposed method

We would like to give an overview of the proposed method. The algorithm steps for the whole procedure are:

1. Calculate the orientation and the intensity variation for each pixel based on Hessian information.
2. Correct the orientation and fill in the dark shadows next to the linear structures.
3. Apply the adaptive multi-scale morpho-Gaussian filter:
 - (a) In a rectangular window, enhance each linear feature and suppress noisy features.
 - (b) Use the multi-scale anisotropic Gaussian kernel to smooth linear features.
4. Calculate the Hessian measurement to further enhance the linear structures.
5. Junction enhancement:
 - (a) Detect the junction center points and branch orientations.
 - (b) Enhance along each branch.
 - (c) Normalize the branches and combine them with the surroundings.

The detailed descriptions for each of the steps will be given in the following sections.

4. Linear feature enhancement

4.1. Hessian measurements and preprocessing

Hessian matrix involves the second order gradient of images. Analysis of the eigenvalues of a Hessian matrix can provide a measurement for the principal direction and the vesselness of a linear structure. Assuming the two eigenvalues of the Hessian matrix of a 2D image are λ_1 and λ_2 , and they satisfy $|\lambda_1| < |\lambda_2|$ (assuming bright structures). The eigenvalues represent the variation of the intensity in a linear structure's principal orientation and its perpendicular orientation. So for a linear structure, $|\lambda_2|$ should be much larger than $|\lambda_1|$. $|\lambda_1|$ should be close to zero. Frangi et al. proposed a linear feature enhancement filter using the numerical relationship between λ_1 and λ_2 [12]. They have

$$H_s(x) = \begin{cases} 0 & \text{if } \lambda_2 > 0 \\ \exp\left(-\frac{R_\beta^2}{2\beta^2}\right)\left(1 - \exp\left(-\frac{S^2}{2c^2}\right)\right) & \text{otherwise} \end{cases} \quad (1)$$

where x is the location of the filter; $R_\beta = |\lambda_1|/|\lambda_2|$ is a blobness measure; S equals $\sqrt{\sum_{j=1,2} \lambda_j^2}$; and β and c are manually set constants. This vesselness measure is analyzed at different scales, s . The maximum response over all the scales will match the width of the linear feature. The principal orientation of the linear structure can be obtained from the eigenvectors. We notice that the large absolute eigenvalue $|\lambda_2|$ corresponding to the maximum-response scale can be used as a measure for the vesselness. It shows the magnitude of the intensity variation in the orientation perpendicular to the principal orientation. This is a good measurement for the likelihood of linear structures. In linear structures, the intensity change along the principal orientation is much smaller than that along its perpendicular orientation. We denote the larger absolute eigenvalues which represent the intensity variation in the perpendicular orientation with V .

As the ends of linear structures do not have obvious or enough linear structure around them, the calculated orientation in this part may be incorrect if the linear structure is thick. The incorrect orientation information will affect the results afterwards. We improve the algorithm developed in [43] so that we can detect the ends of the linear structures, and we correct the orientation of this part by an updated orientation. In the junction detection method described in [43], we set a lower threshold for the initial candidate points selection and allow junctions to have only one branch. The orientation of the branch is also detected. Then we replace the orientation of the ends with that of the branch. We show the corrected orientation in Fig. 1. We can see that the ends of the linear structure are corrected. The corrected orientation field is denoted with O . The two measurements, V and O , will be used later.

The intensity across the linear feature is supposed to be similar to a Gaussian-shape. In some images, due to optical aberration or noise, a dark shadow sometime appears beside the linear features. The shadow will influence the morphological operation afterwards, enlarging the black shadow. In our work, an operation is carried out to solve this problem. We fill in the dark shadow in the direction perpendicular to the linear feature. For an arbitrary pixel p , we check the intensity profile along the orientation perpendicular to O_p (the angle at p). If there is a concavity along the intensity curve, we replace the concave part with a larger value next to it. Then the concave part is filled and smoother linear features are obtained (see Fig. 2).

4.2. Multi-scale morpho-gaussian filter and hessian measurement

4.2.1. Adaptive morphological enhancement

Tankeyevych et al. [24] proposed a novel opening operation and enhanced the linear structures along each pixel's orientation. In their erosion (or dilation, depending on whether the foreground is bright or dark) step, assuming $B(p)$ is a linear structure element around pixel p and along p 's orientation, the intensity values of pixels in the structure element $B(p)$ that are lower than that of p will be replaced with p 's intensity. Then a dilation operation is carried out. This method iteratively changes one pixel's intensity with larger values if this pixel is within several structure elements and if it is not brighter (or darker) than the center pixel. Therefore a reconnection of broken lines can be achieved. However, this method does not have too much effect on noisy pixels, as the pixels in its neighborhood will also be enhanced. Moreover, their method cannot smooth the linear structures if the intensity is unevenly distributed.

In our algorithm, we use the Hessian measurement V which represents the intensity variation in the direction perpendicular to the linear feature to reduce noise and we propose an adaptive linear directional morphological operation (for bright linear structures) along each linear structure. For an arbitrary pixel p in the image, the linear structure element $B(p)$ (with length L) for p is centered at p and oriented in orientation O_p . We check p 's perpendicular intensity variation V_{pi} for all the pixels in $B(p)$ as V_{pi} measures the likelihood of a linear structure for one pixel. We define a ratio γ as the number of pixels with small V (smaller than a threshold ζ) to the length of the structure element. That is: $\gamma = \text{number}_{V_{\text{small}}} / L$. If the value V for a pixel q in $B(p)$ is smaller than the threshold ζ , it will be considered as a pixel with V_{small} . If γ is larger than γ_{thresh} (here we set γ_{thresh} to 90%, and this threshold is kept constant), it means that the pixels in the structure element are not located along a linear structure. Then if the intensity at q is larger than that at p , we replace the intensity at q with that at p . So the bright pixels of noisy structures will be suppressed. If the ratio does not reach γ_{thresh} , it shows that $B(p)$ may be inside a linear structure, although some weak signals may exist. Therefore, an

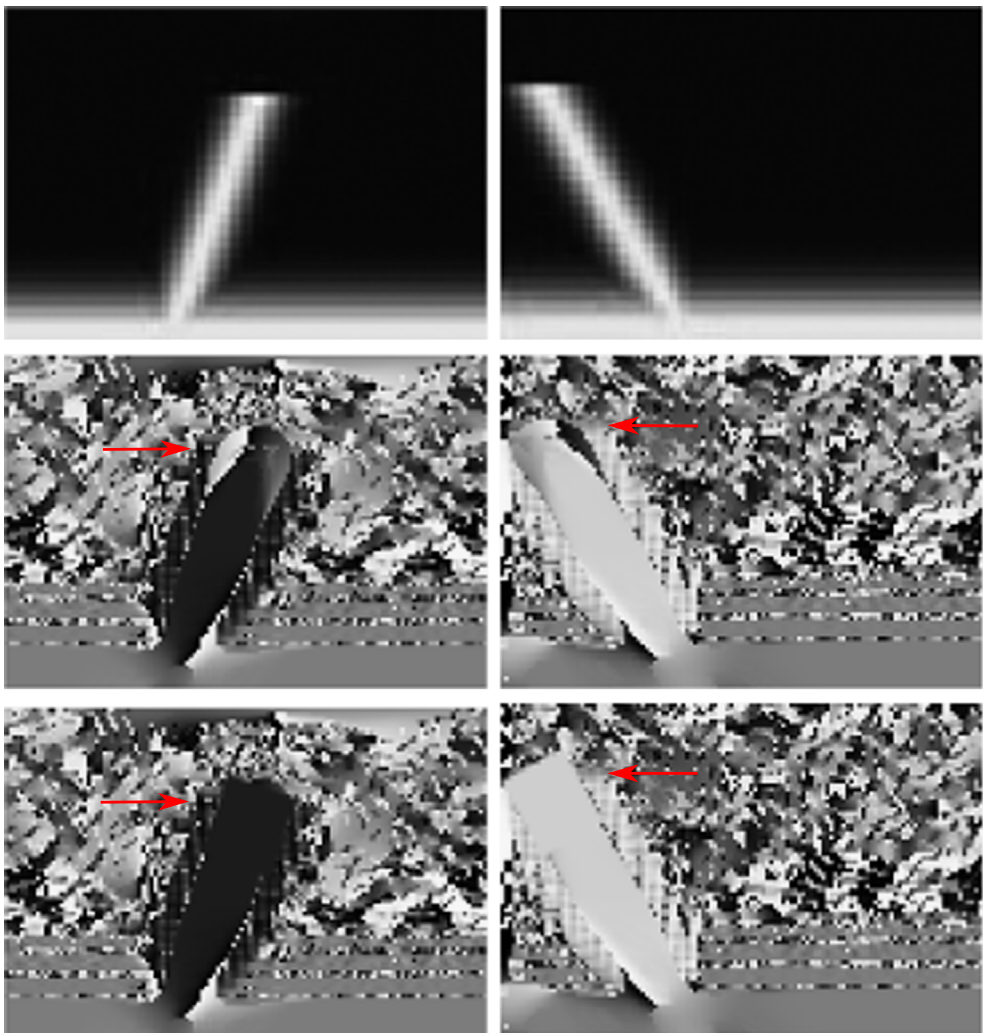


Fig. 1. Two examples showing orientation correction. The value of a pixel represents the direction for that pixel. The first row is the input structure. The second row is the orientation calculated from the Hessian method. The third row is the orientation after correction. The two columns are two end structures from two long linear features. It can be seen that the orientation before correction is affected by the background, and wrong orientations are obtained. After correction, the orientations in the end parts have similar values with the linear structures where they belong to.

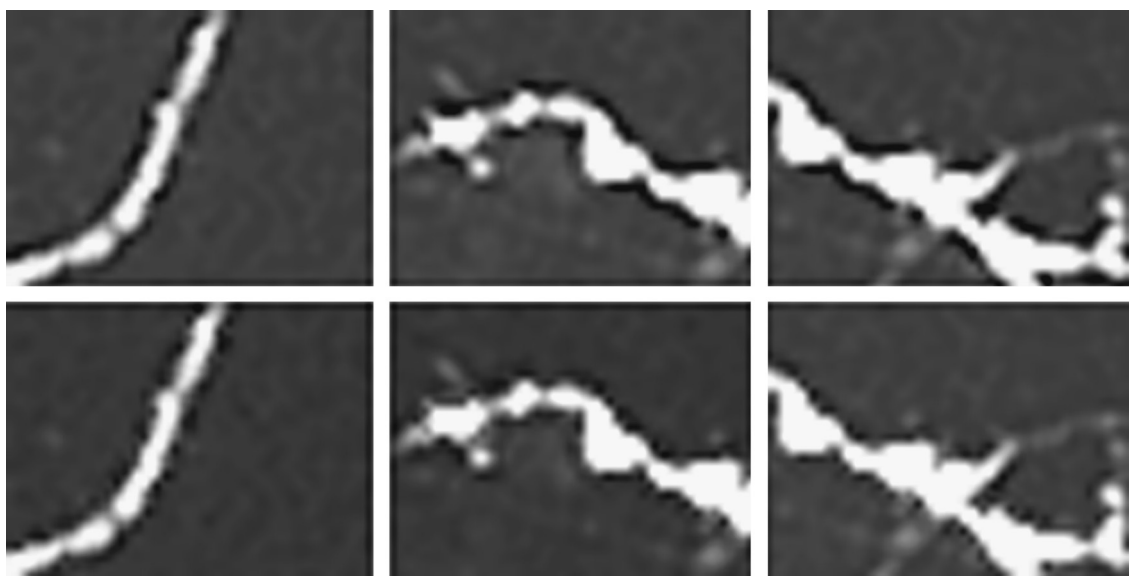


Fig. 2. Three examples showing shadow preprocessing. The top row is the input image. The bottom row is the output image. We can see that the dark shadows beside the linear features are removed or greatly reduced.

enhancement needs to be carried out. If the intensity at q is smaller than that at p , it will be replaced with the intensity at p . The adaptive morphological operation achieves an enhancement for linear structures and a suppression for noisy structures.

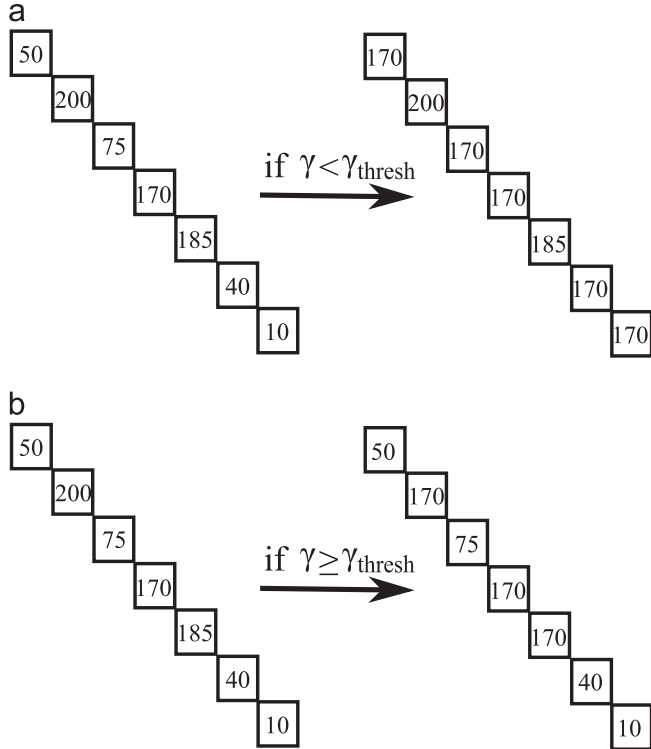


Fig. 3. An illustration for the adaptive linear morphological operation. We assume that the structure has seven pixels. (a) if $\gamma < \gamma_{\text{thresh}}$, the center pixel's intensity is used to replace the lower intensity; (b) if $\gamma \geq \gamma_{\text{thresh}}$, the center pixel's intensity is used to replace the higher intensity.

The morphological operation is consequently

$$I(b) = \begin{cases} \sup(l(x+b), I(x)) & \text{if } \gamma < \gamma_{\text{thresh}} \\ \inf(l(x+b), I(x)) & \text{otherwise} \end{cases} \quad (2)$$

where $I(b)$ is the intensity value in the structure element; $\sup()$ and $\inf()$ represent supreme and infimum respectively.

This proposed adaptive morphological enhancement along one orientation dilates or erodes the structures according to the property of the structure. Using this filter, the linear features will be enhanced and noise will be suppressed. Moreover, this morphological operation can reconnect any broken linear features and enhance weak signals. We show the process of the operation in Fig. 3.

4.2.2. Smoothing and enhancing with an oriented anisotropic Gaussian kernel

To solve the problem of unevenness of the surface of the linear structures, we need to find a function which can smooth as well as enhance the linear feature along its orientation. Because of the similarity of a Gaussian function and the cross section of linear features, multi-scale 2-D oriented anisotropic Gaussian templates are convolved with the morphological enhanced images for the purpose of smoothing and enhancement. The anisotropic Gaussian function has the following form:

$$h(x, y : \phi, f) = \exp \left\{ -\frac{1}{2} \left[\frac{x_\phi^2}{\sigma_x^2} + \frac{y_\phi^2}{\sigma_y^2} \right] \right\} \quad (3)$$

with

$$\begin{cases} x_\phi = x \cos \phi + y \sin \phi \\ y_\phi = -x \sin \phi + y \cos \phi \end{cases} \quad (4)$$

The anisotropic Gaussian kernel has two parameters: σ_x and σ_y . We set $\sigma_y = k * \sigma_x$ and $k \geq 1$ as the linear feature's length should be larger than its width. The shape of the Gaussian kernel is shown in Fig. 4. From the figure, we can see that the function has a Gaussian shape in both the principal orientation and the orientation perpendicular to it. But the width in the perpendicular direction is smaller than that in the principal direction. As mentioned,

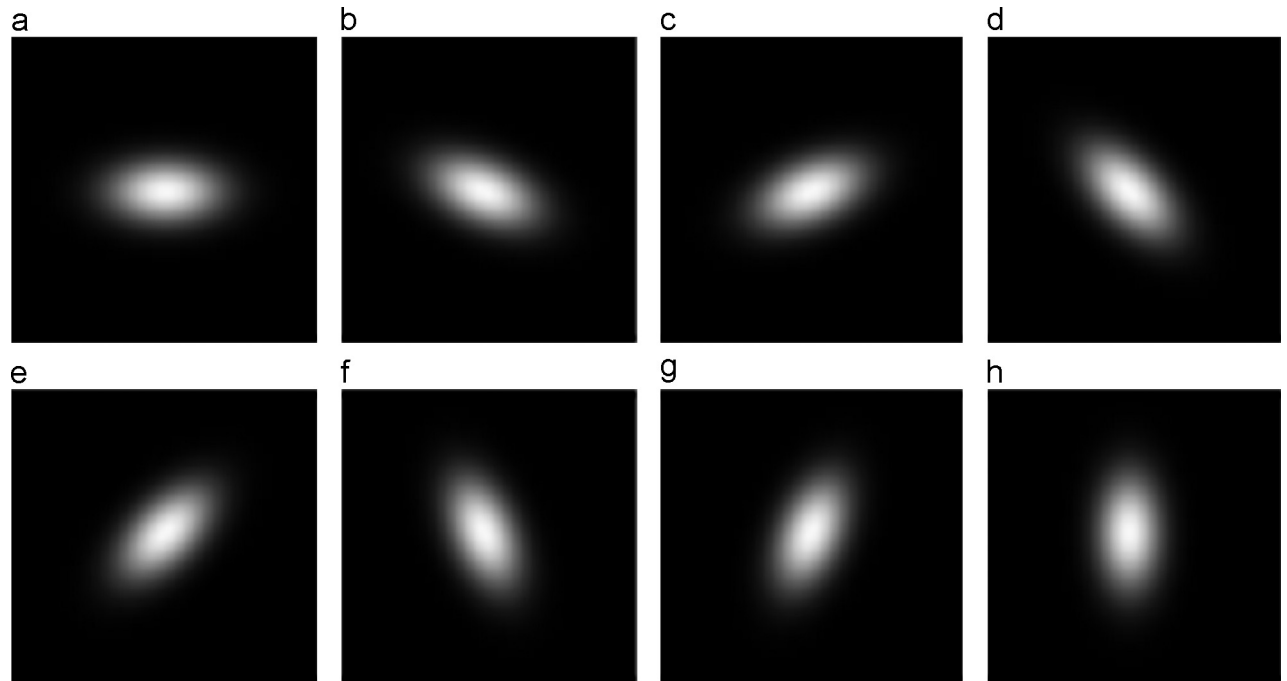


Fig. 4. Anisotropic Gaussian kernel in eight orientations in a single scale. From (a) to (h), the orientations are: $0, \pi/8, -\pi/8, \pi/4, -\pi/4, 3\pi/8, -3\pi/8$, and $\pi/2$.

to capture the linear features with variable widths, the linear feature measure in Eq. (3) is analyzed at different scales. So multiple σ_x values are used in order to obtain the largest response. When the response reaches its maximum at one scale, it shows that the width of the linear structure matches the scale. Hence the maximum response will be chosen as the filtered output.

4.2.3. Multi-scale morpho-Gaussian filter and Hessian measurement

Based on what we have described, we can apply the morpho-Gaussian filter on each pixel. For an arbitrary pixel p , we carry out the morphological enhancement operation for each pixel in a small rectangular window along angle O_p . In the local window, all the linear structures are enhanced and the non-line structures like noise or blob structures are suppressed. Next, we carry out the Gaussian smoothing in the local window centered at p . The convolution for the small window with the oriented anisotropic Gaussian kernel is calculated according to the following equation:

$$G(x, y) = g_{\phi, s}(x, y) * E(x, y) \quad (5)$$

where $G(x, y)$ is the response; $g_{\phi, s}$ is the anisotropic Gaussian kernel at angle ϕ and scale s ; $E(x, y)$ is the enhanced image in the small window. '*' is the convolution operation. Multiple scales are used to match the structures with variable widths.

After this operation, enhanced as well as smoothed linear features are obtained. We give two examples in Fig. 5 to show

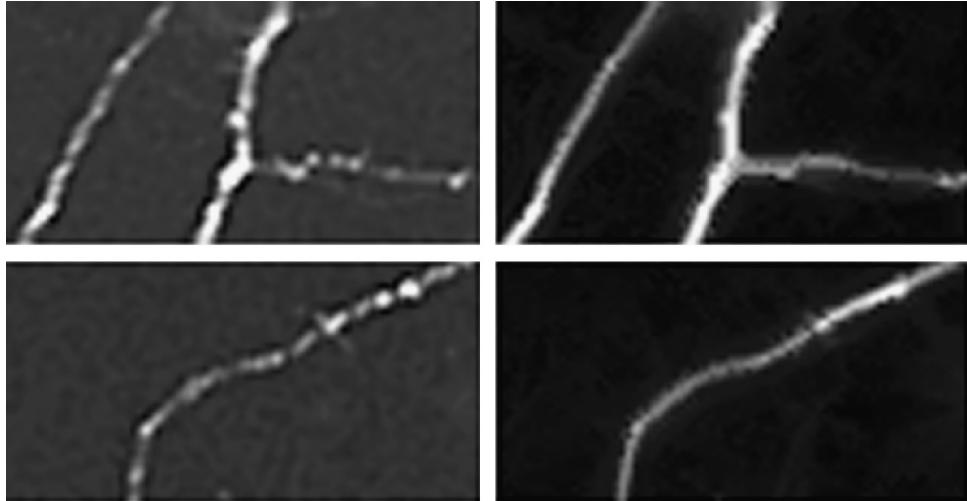


Fig. 5. Two examples of linear feature enhancement. The left column is the input images and the right column is the output images. From the images, we can see that the weak signals are enhanced and the uneven parts are smoothed.

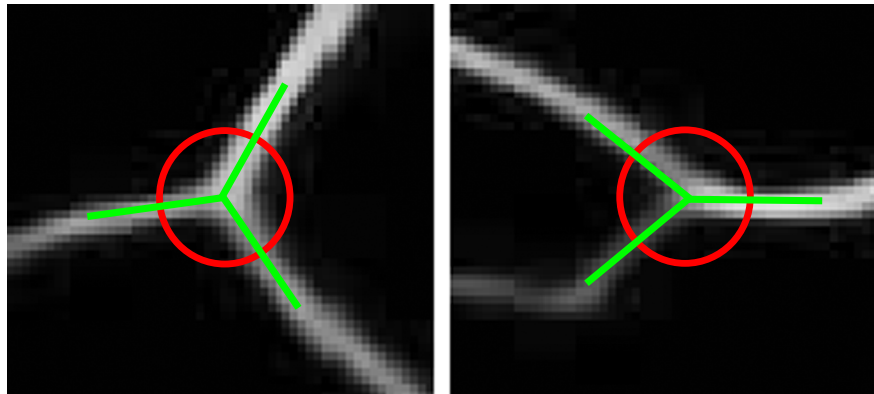


Fig. 6. Two examples demonstrating the junction detection results. The red circles are the regions of the junction; the center of the circle is the junction center point; the green lines represent the orientation of the branches. (For interpretation of the references to color in this figure caption, the reader is referred to the web version of this article.)

the enhancement results, where the weak signals are enhanced and the linear features are smoothed by using our algorithm.

A Hessian measurement is used here to further reduce the noise. We use the following measurement:

$$H'_s(x) = \begin{cases} 0 & \text{if } \lambda_2 > 0 \\ |\lambda_2| & \text{otherwise} \end{cases} \quad (6)$$

We select the largest response among multiple scales. Our measurement is less 'strict' as the blobness measurement is not included, so the junction suppression is largely reduced. The filter further enhances the linear structures.

5. Junction enhancement

Junctions are the regions where three or more linear structures meet. We call these linear structures at junction regions 'branches'. Hessian-based methods such as Frangi et al.'s method [12] have a problem of junction suppression [17]. In the proposed method, we do not have the junction suppression problem in the morpho-Gaussian filter step as our algorithm only uses the orientation information and the intensity variation from the Hessian matrix. Besides, enhancement of linear features in the local region of the junctions can also enhance the junctions. However, in the step of Hessian measurement, although a measurement which is much less strict than the Frangi et al.'s method is used, the junction

suppression problem still exists. To solve this problem, we first detect the junctions and their branch orientations using the method described in [43]. Then we decompose the junctions, enhance along each branch, recombine the decomposed parts and fit them with the surrounding linear structures. For convenience, we call the image after linear feature enhancement and before junction enhancement I_{lj} .

Su et al. [43] used a correlation matrix and a Hessian matrix to determine the initial candidate junction points. Then junctions are detected using the intensity and shape information. In junction regions, three or more intensity peaks exist within 360 degrees around the center point. A multi-scale Gaussian template is used to match with the potential branches of each junction. The pixel with the largest matching score is the center point for one

junction. As mentioned in Section 4.1, the end points of linear features can also be detected via this method by setting a small threshold for the initial candidate points and setting the junction branch number to 1. Both junctions and end points can be detected using this method. We show two examples of junction detection results in Fig. 6.

Now the junction center points and branch orientations are obtained. For a junction center point, assuming it has three branches, we cut the junction region into subimages and decompose the junction region into three parts. Each branch is included in each part. The dividing lines are angular bisectors between two neighboring branches. Then we enhance each of the branches along its orientation. In this step, we regard the junctions as three individual linear structures. We firstly enhance the branches with

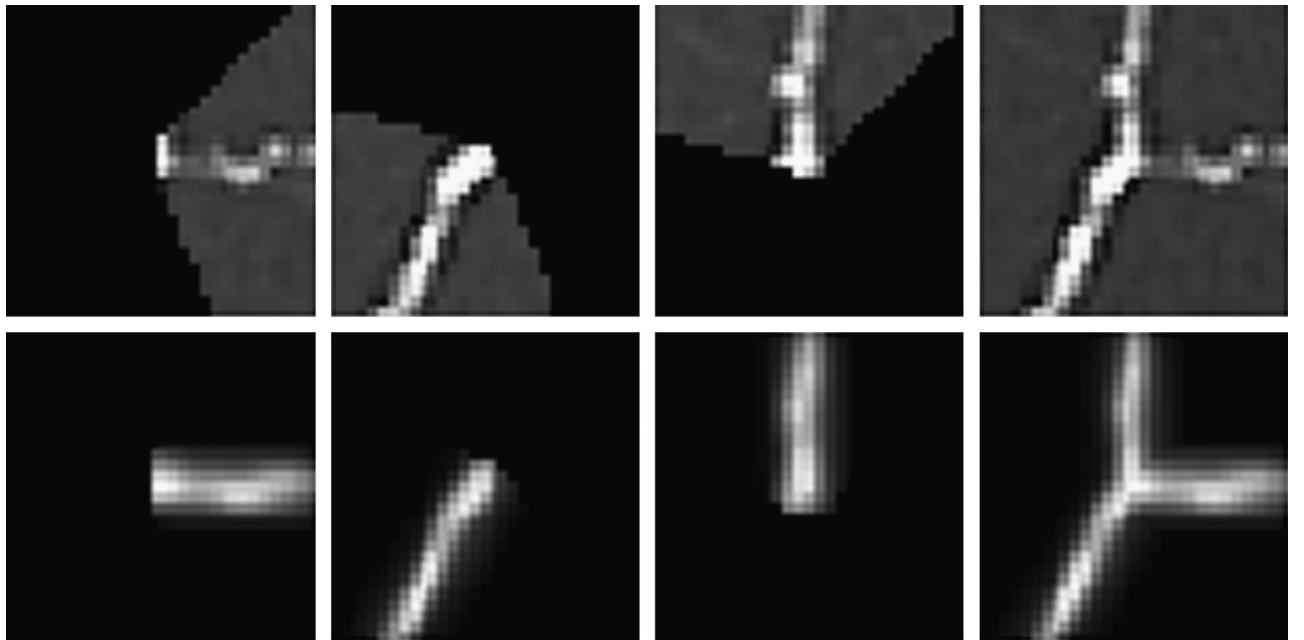


Fig. 7. An example showing junction enhancement result. In the top row, the first three are the decomposed parts of the fourth one; the bottom row is the enhancement branches. The last one of the bottom row is the recombined enhanced result.

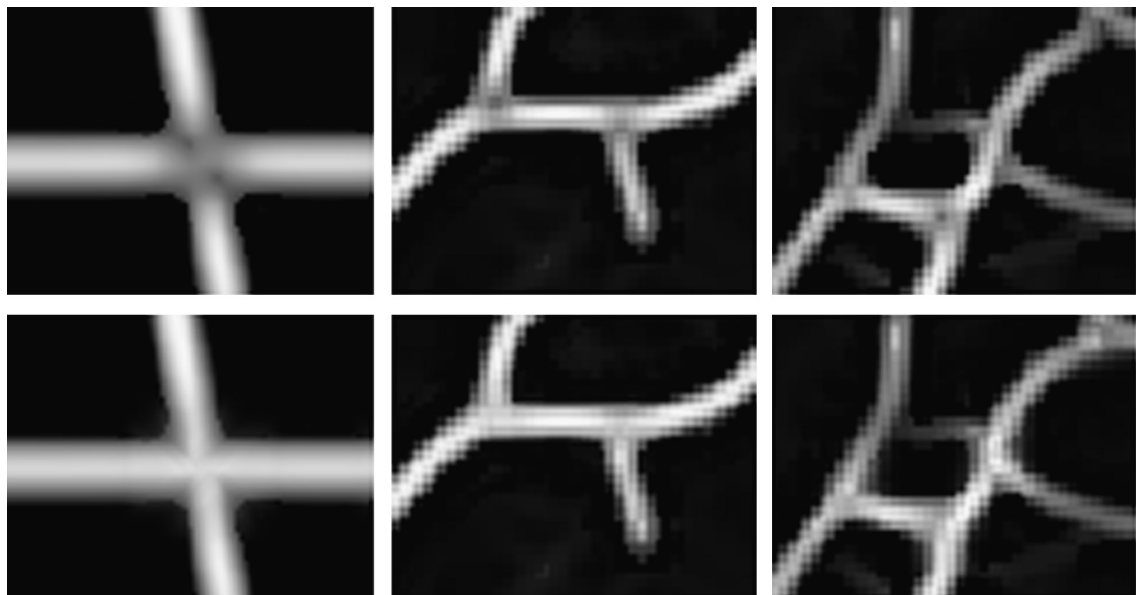


Fig. 8. Three subimages showing junction enhancement. The top row is the result after linear feature enhancement. The bottom row is the result after junction enhancement.

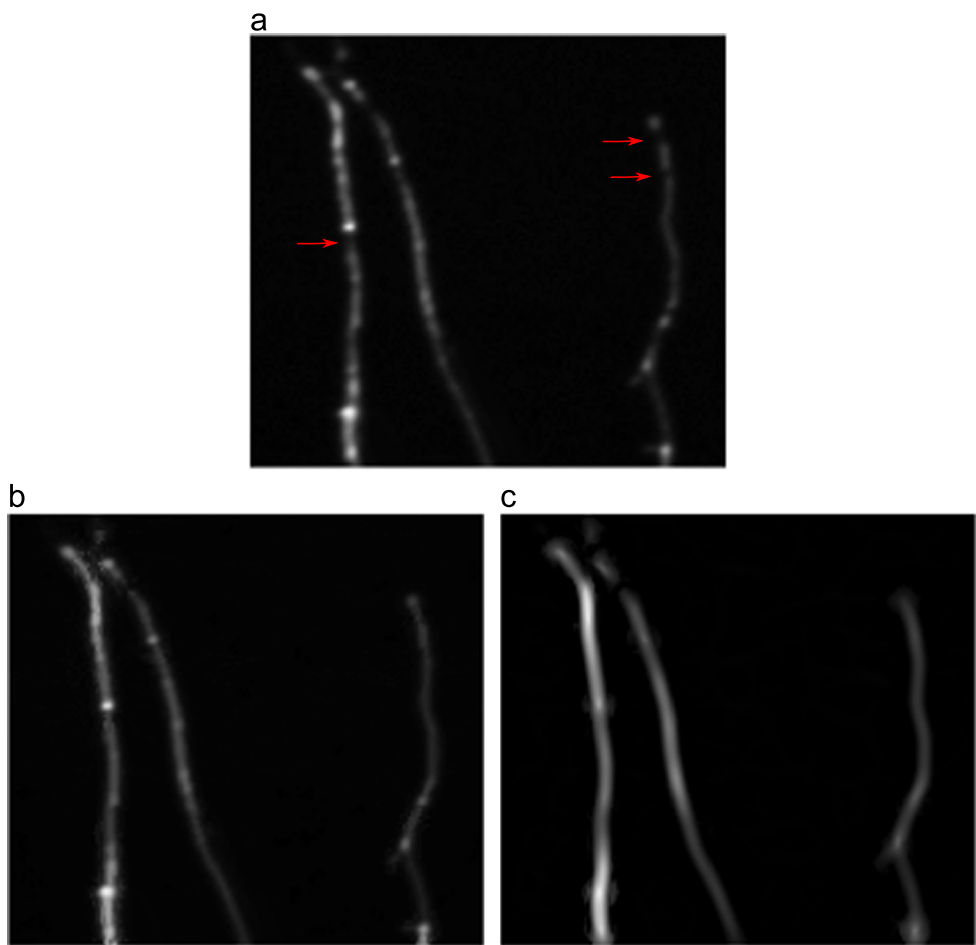


Fig. 9. An example showing our enhancement result and Tankyevych et al.'s method. (a) is the input image; (b) is the result using Tankyevych et al.'s approach; (c) is the output image using the proposed method.

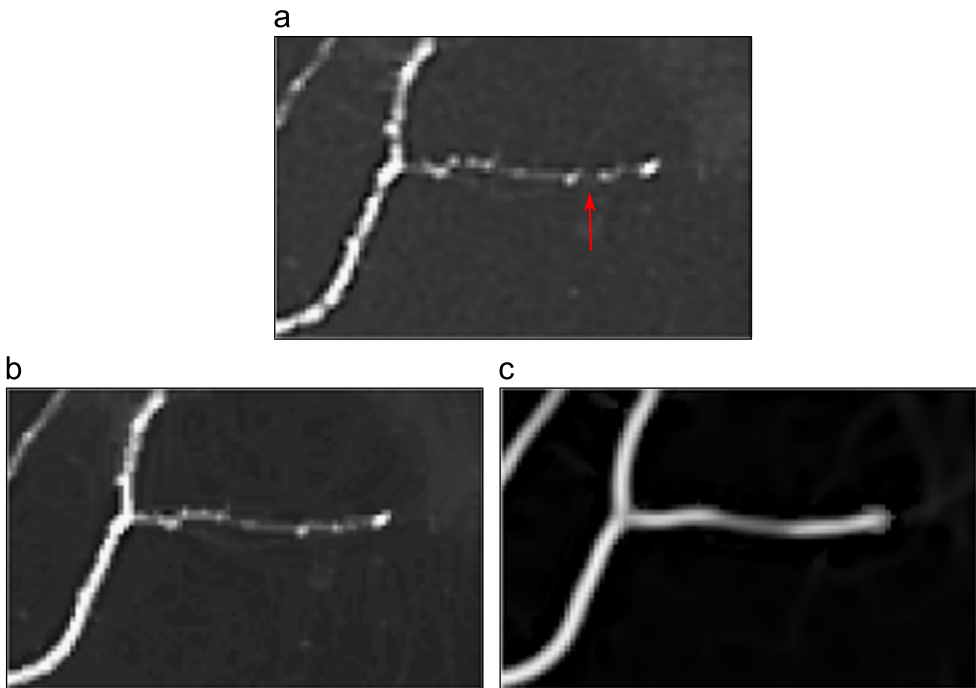


Fig. 10. Another example showing our enhancement result and Tankyevych et al.'s method. (a) is the input image; (b) is the result using Tankyevych et al.'s approach; (c) is the output image using the proposed method.

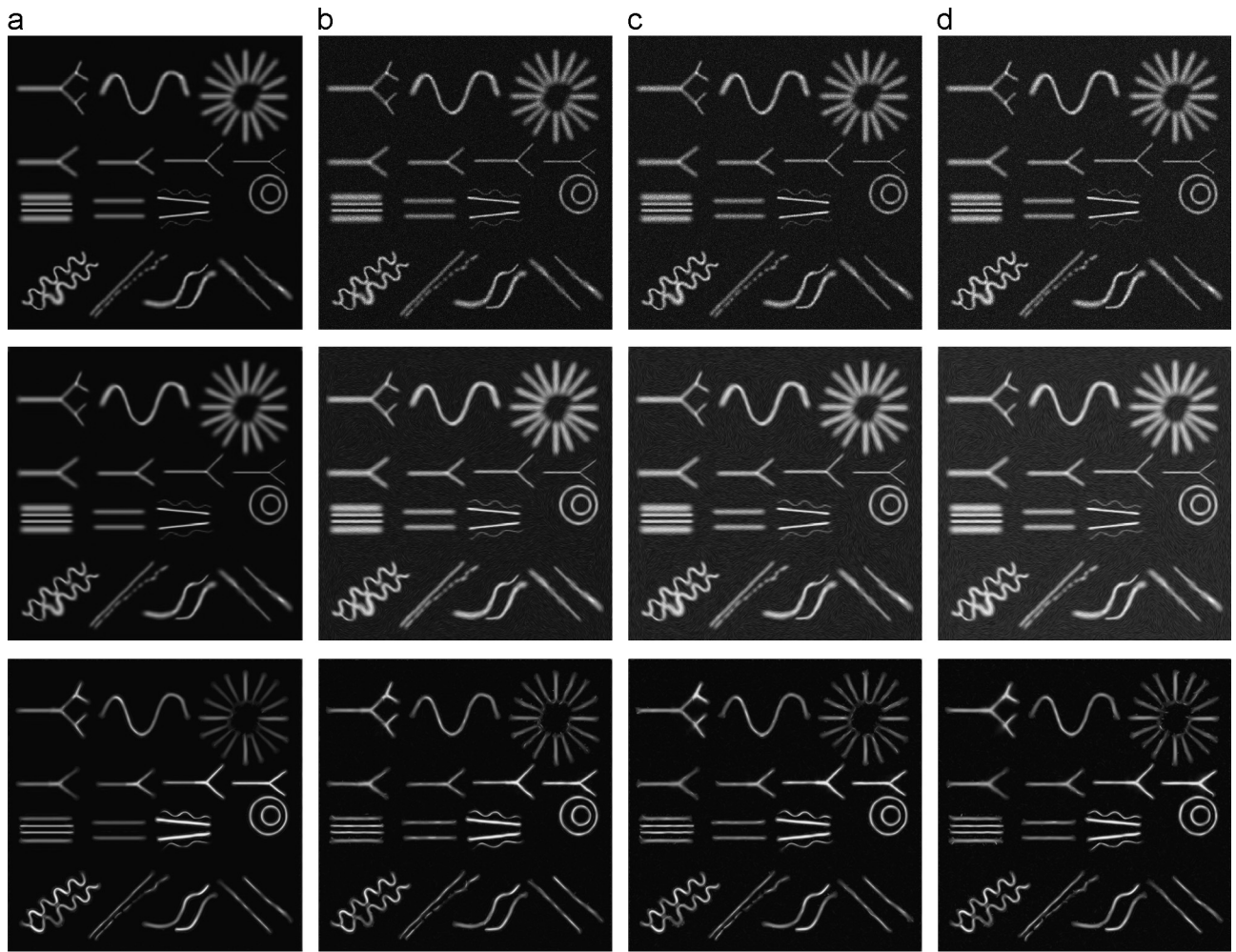


Fig. 11. The comparison between Kroon et al.'s method and the proposed method. The first row is the input images. The second row is the results using Kroon et al.'s method. And the third row is the results using the proposed method. The input in column (a) is the image without noise; the input in (b) is the image with 0.04 Gaussian noise; (c) is the image in (a) with 0.08 Gaussian noise and (d) is the input in (a) with 0.12 Gaussian noise.

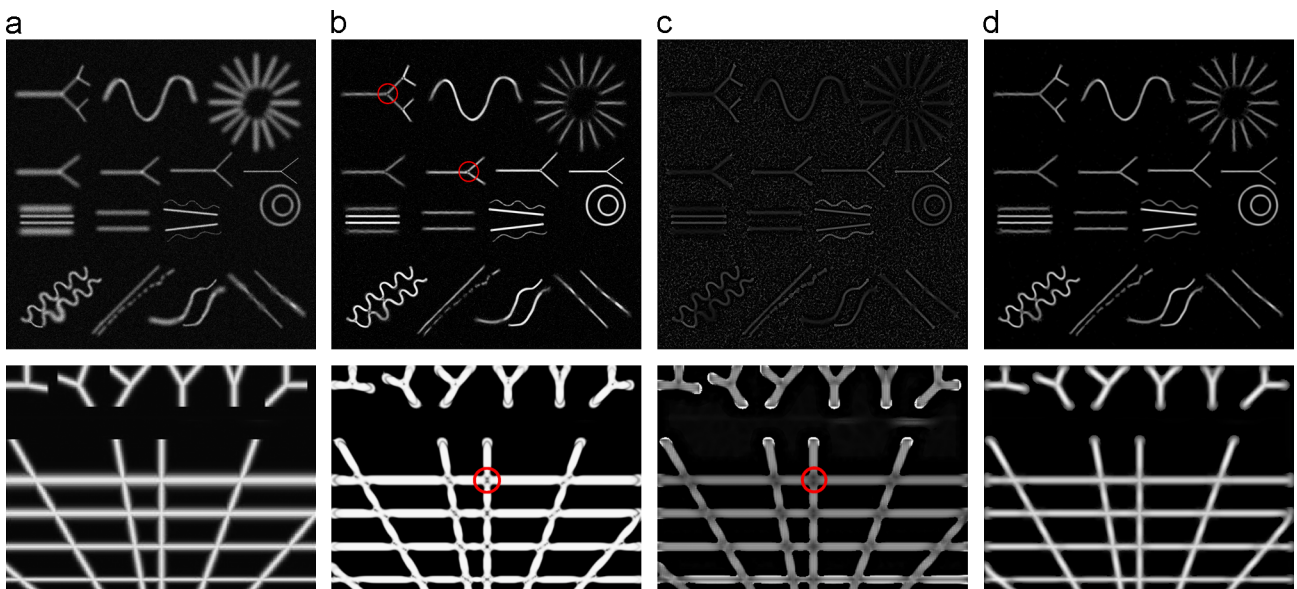


Fig. 12. The comparison among the proposed method, Frangi et al.'s filter and Shikata et al.'s method. The top row and bottom row are two synthetic images. (a) is the input images; (b) is the results of Frangi et al.'s method; (c) is the results of Shikata et al.'s method and (d) is the results of the proposed method.

morphological operations, then we carry out the oriented multi-scale Gaussian enhancement, which is shown in [Section 4.2.2](#). Through this step, the weak signals in the branch can be enhanced and the extremely bright signals will be dimed. We show an example in [Fig. 7](#). We can see that the junctions are smoothed and enhanced. Next, the three branch regions are recombined, which is shown in the last image in the second row of [Fig. 7](#). After recombination, the subimages should have a good fit with I_{lj} . Otherwise there will be an obvious difference between the subimages and its surroundings. The pixels in the subimages are normalized with respect to the intensity range according to its neighborhood in image I_{lj} and then re-inserted into the image. This ensures that separated parts have a good fit with its surroundings. Two examples of enhanced junctions after recombination and fitting with their surroundings are shown in [Fig. 8](#). From the images, we can see that the junctions are much better enhanced than only using the linear feature enhancement.

6. Experimental results and comparisons

We evaluate the performance of the proposed method through applications to 49 images which include synthetic images, neurite images, leaf vein images and retinal images. We compare our results with four other methods: Tankyevych et al.'s method [24], Kroon et al.'s method [22], Frangi et al.'s method [12] and Shikata et al.'s method [15]. The reason we choose these four methods is that Frangi et al.'s method and Shikata et al.'s method are two classic Hessian methods for linear feature enhancements. The Tankyevych et al.'s method has very good performance in terms of reconnection and recovery; Kroon et al.'s method is good at noise removal. In the following sub-sections, we give reconnection comparison results with Tankyevych et al.'s method and noise removal comparison with Kroon et al.'s method. Then we compare our method with Hessian based Frangi et al.'s and Shikata et al.'s methods in [Section 6.3](#) and give statistical results.

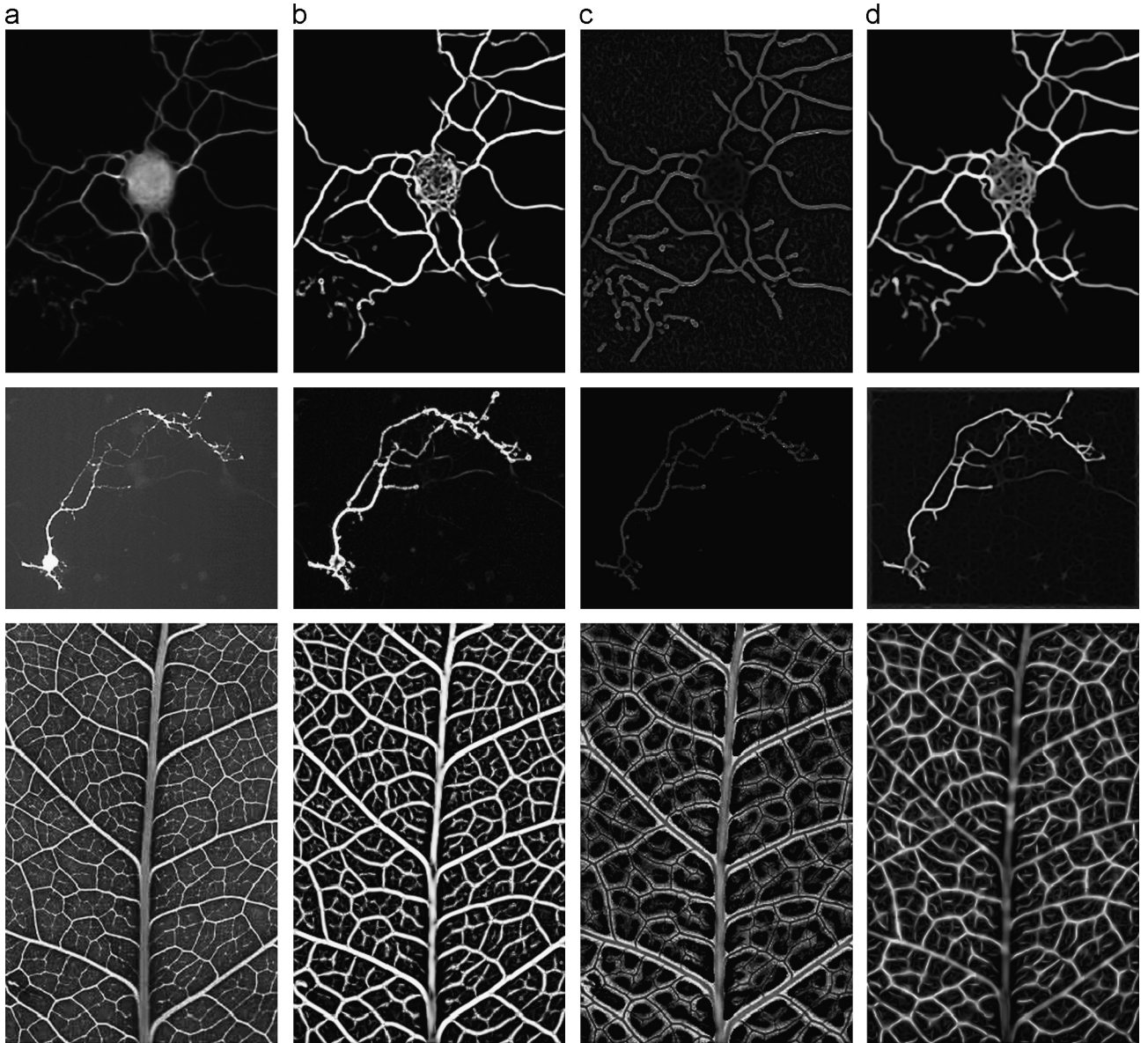


Fig. 13. The comparison among the proposed methods, Frangi et al.'s method and Shikata et al.'s method. The top row and second row are two neurite images, and the bottom row is the leaf vein images. (a) is the input images; (b) is the results of Frangi et al.'s method; (c) is the results of Shikata et al.'s method; and (d) is the results of the proposed method.

6.1. Reconnection and recovery comparison

In this section, we compared the proposed method with Tankyevych et al.'s method. Tankyevych et al.'s method is known for its recovery capability. The proposed method, which is applied in a rectangular window, uses multi-scale morpho-Gaussian filter to enhance and smooth linear structures. Then a Hessian enhancement is carried out to further enhance the linear structures. Therefore, our filter can enhance the linear structures and make the linear structures smoother.

We show two example results in [Figs. 9 and 10](#). The broken parts of the linear structures are marked with red arrows. Both the proposed method and Tankyevych et al.'s method can reconnect and enhance these parts, yet the proposed method show a great improvement as it is more adaptive to different features. The Tankyevych et al.'s method reconnects the broken parts through morphological opening along the linear structure's orientation. Similarly, the proposed approach enhances the linear structure through morphological operation, but it is based on the structure's 'lineness', measured by the combination of Hessian measurements. So the proposed method is more accurate and has a better recovery performance. Then the anisotropic Gaussian smoothing along the principal orientation and Hessian enhancement both make the feature much smoother. The intensities of the extremely bright parts are reduced and the dark parts are enhanced.

6.2. Noise removal comparison

Kroon et al. employed the anisotropic diffusion filtering to remove noise and enhance the mandibular canal in CBCT

scans [\[22\]](#). The diffusion equation has the form as following:

$$I_t = \nabla \cdot (D \nabla I) \quad (7)$$

where D is the diffusion tensor. They introduced a novel discretization scheme of the anisotropic diffusion tensor based on a cost function. The scheme is optimized for rotational invariance. This method has been highly evaluated for noise removal, so we compare the proposed method with theirs in terms of noise removal capability.

Kroon et al.'s method iteratively smoothes the images using the optimized diffusion scheme and it can preserve the linear features well. However, the proposed method performs better in terms of noise removal. From [Fig. 11](#), as noise increases, the Kroon et al.'s method performs worse. But the proposed method is only slightly affected by the noise. The reason is when the adaptive multi-scale morpho-Gaussian filter processes the images, it will automatically enhance the linear features and suppress the noisy pixels according to each pixel's lineness measurement.

6.3. Comparison with Hessian-based method

In recent years, a number of enhancement methods were proposed based on Hessian information. We selected three classic methods for comparison. We have described Frangi et al.'s method in a single scale. When multiple scales are used, the largest response is selected, that is

$$H_0(x) = \max_{s_{\min} \leq s \leq s_{\max}} \{H_s(x)\} \quad (8)$$

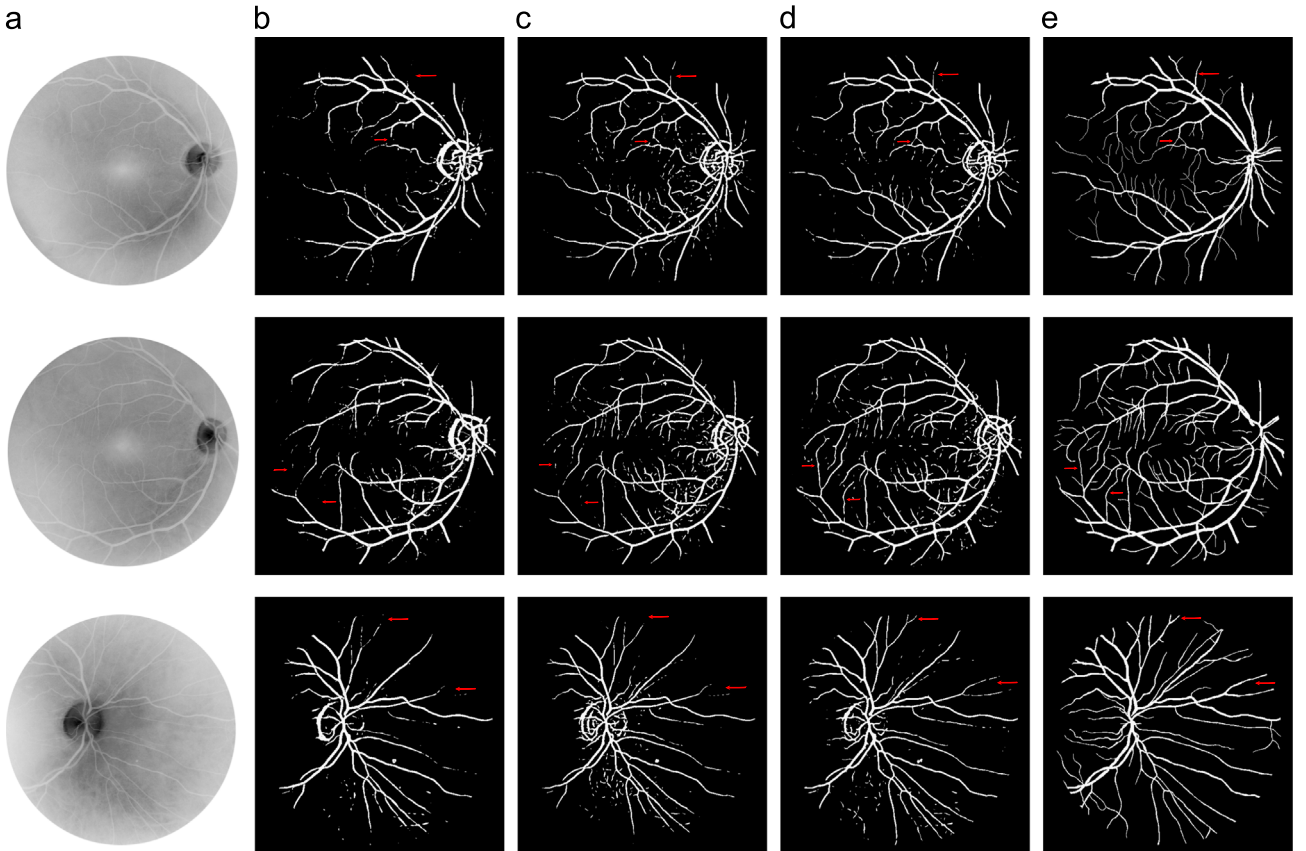


Fig. 14. The three rows are three different images randomly chosen from the DRIVE dataset. They were processed using three enhancement filters and then segmented using global thresholding. (a) is the input images; (b) is the results of Frangi et al.'s method; (c) is the results of Shikata et al.'s method; (d) is the results of the proposed method; (e) is the ground truth images.

In Shikata et al.'s approach, the single scale filter is

$$H_s''(x) = \begin{cases} 0 & \text{if } \lambda_2 > 0 \\ \frac{s^2 |\lambda_2|}{I(x)} & \text{otherwise} \end{cases} \quad (9)$$

where $I(x)$ is the intensity value at location x . The largest response corresponding to one scale is chosen as the filter output using Eq. (8).

We show the enhancement results in Figs. 12 and 13. The input image in the top row of Fig. 12 was obtained from www.ecse.rpi.edu/censis/phantom. The input image in the bottom row of Fig. 12 was obtained and adapted from [25]. Contrast and brightness of the images are adjusted for better display. Fig. 12 shows the results of two synthetic images. The first row is a synthetic image which is obtained with 1% Gaussian noise added to the original image. Note the parts of the junction region (we marked several examples in the figures with red circles) in Frangi et al.'s and Shikata et al.'s methods, these parts are always suppressed in their methods. Our method addresses this drawback and obtains a much cleaner and smoother result. Here the structure element in the morph-Gaussian filter is set to 11 so that the two structures (the two structures in the left bottom corner in the first image) which are too close to each other will not be connected after enhancement. Therefore the gap in the linear structure (next to the structures

mentioned above) will not be filled. In real applications, gaps can be filled by setting proper length for the element structures. There are two neurite images and one leaf vein image in Fig. 13. From these three images, we can see that the Frangi et al.'s method and the Shikata et al.'s method lose some tiny structures, and they cannot smooth the uneven features. Both of these two methods have a problem of junction suppression, while our junction enhancement method can solve this problem.

For a better comparison and quantitative analysis, we tested the three methods on forty retinal images in the DRIVE database [44] and observed the results. The scales we used for the three methods are $\sqrt{2}/2, \sqrt{2}, 3\sqrt{2}/2$, and $2\sqrt{2}$. We segmented the images after three enhancement methods for quantitative analysis. A global threshold method from a small threshold value to a large threshold value on all the enhancement results is carried out. The manual segmentation mask in the database were used as the ground truth. We use the mean square error (MSE) between the segmentation results and the ground truth to measure the enhancement result [25]. This value was calculated by the sum of intensity differences of the corresponding pixels which was then normalized by the size of the ground truth data. The smaller the value is, the less different between the mask and the segmentation result will be. So a smaller MSE demonstrates a better result. We choose the result which gives the smallest MSE among all the global thresholds' results for each image as the final result. We show three segmentation examples in Fig. 14 and the average MSE values for all the test data in Table 1. We also plot the histogram of MSE for each image in Fig. 16. To better show the results, We apply a pseudo-Euclidean skeletonization to the segmentation results [30] and the skeletons of the segmentation results are shown in Fig. 15.

Table 1
Average MSE values for three methods.

Methods	Frangi et al.	Shikata et al.	Proposed method
Average MSE%	4.27	4.24	3.18

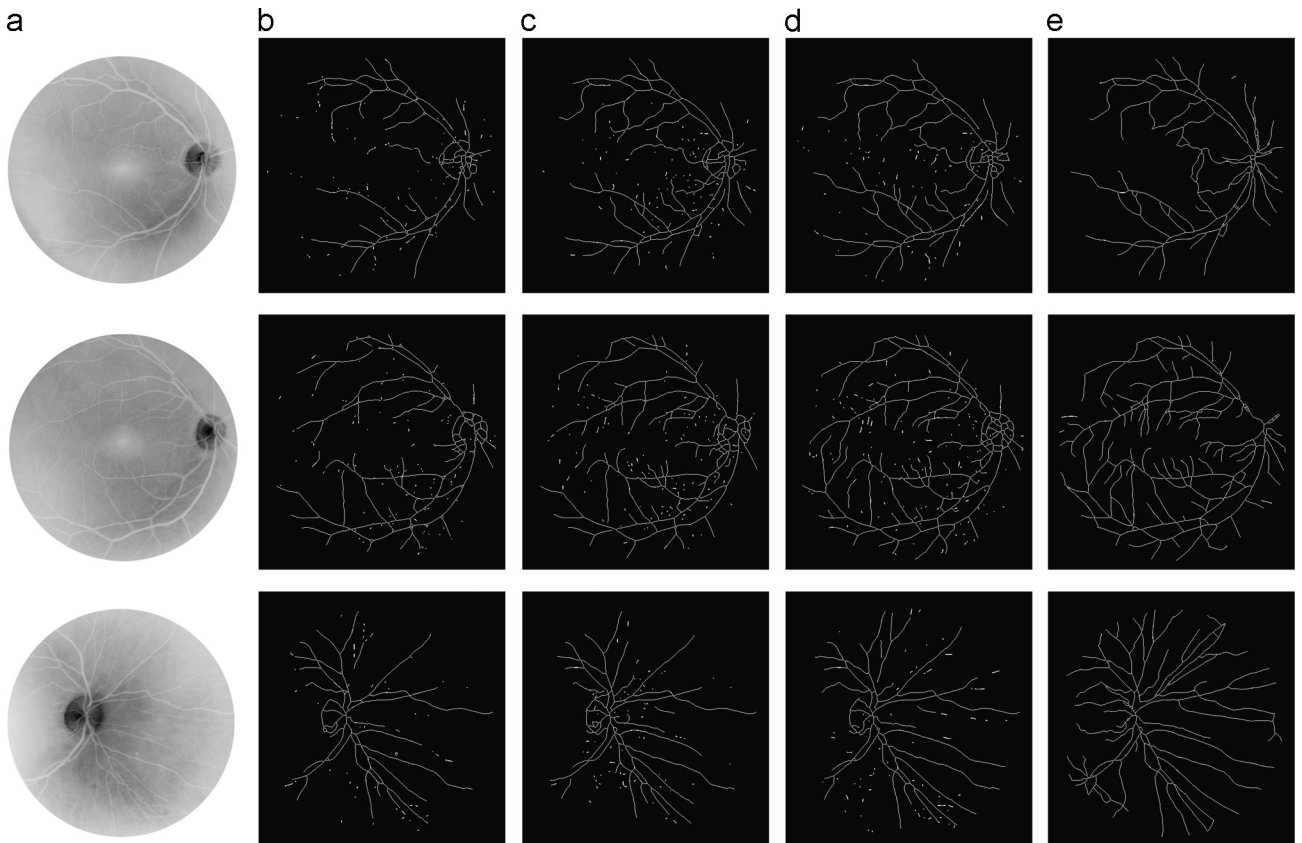


Fig. 15. The skeleton extracted from the segmented images. The two rows are corresponding to the two rows in Fig. 14.(a) is the original input image data, (b) is the extracted skeletons from column (b) in Fig. 14; the skeletons based on Shikata et al.'s methods are shown in (c); (d) is the skeletonization result of the proposed method and (e) is extracted skeletons of the ground truth.

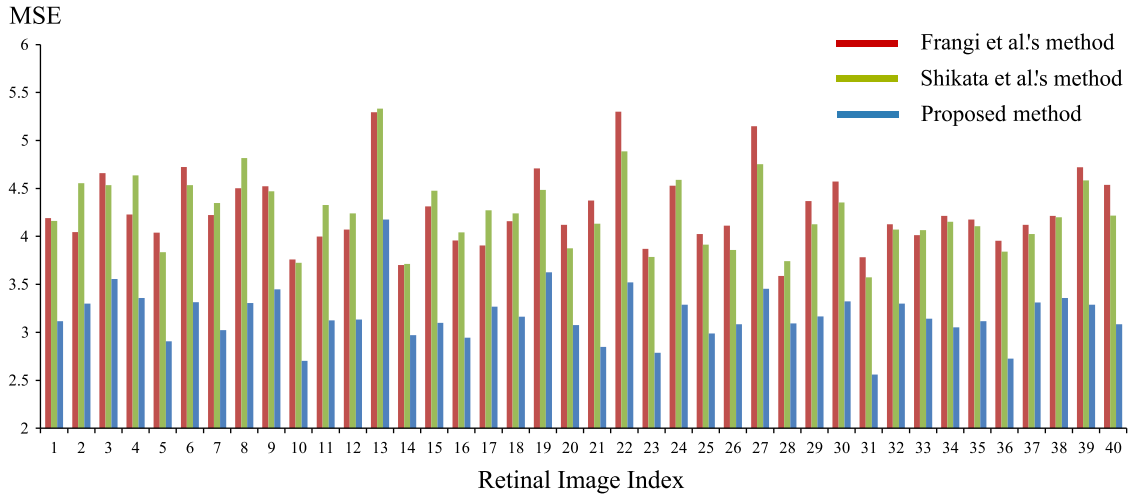


Fig. 16. The histogram of MSE for all the images using three methods. It can be observed that the error of our method is smaller than that of the other two methods.

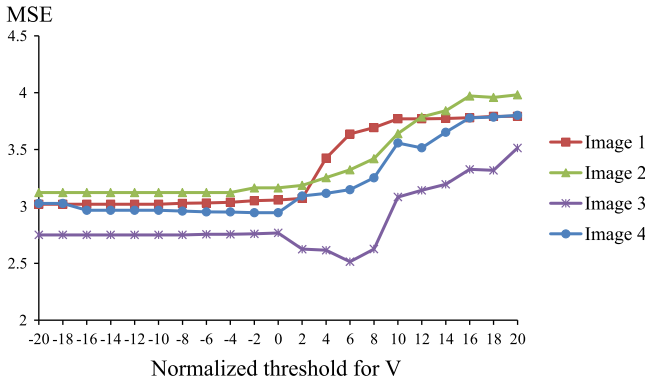


Fig. 17. The MSE value after changing the threshold for V . Four colors represent four images. We set the threshold that we used for all the images to be 0 and calculate the MSE when adopting different options with a fixed interval 2 to test the sensitivity.

From the three examples, it shows that our method can preserve more useful minutiae. We marked some parts of the vessels in the images to show the preservation of the features. Some of the marked vessels are difficult to observe by human eyes due to the low intensity contrast (e.g., the top arrow in the first row), but they can be detected using the proposed method. Furthermore, these tiny and thin vessels are lost in the two other methods, while they are well preserved and enhanced using the proposed method. The skeleton extraction results further show that we can keep more details than the two other methods, which means the proposed enhancement method will greatly improve the centerline extraction results. The better performance of the proposed method is from the adaptive enhancement of the features along their orientations. Besides, sometimes the junction parts become broken using their methods; however, our proposed method does not have this problem. From the table and the graph, we can see that our method has a smallest MSE among the three methods, which shows the result of our method is much closer to the ground truth and our method can enhance the linear structures more efficiently.

There are several parameters in our algorithm: the scales related to the Hessian matrix eigenvalues analysis, the length for the structure element, the window size for the morpho-Gaussian filter, the threshold ζ for V in Section 4.2.1 to judge if it is a dilation operation or an erosion operation and σ_x for the scale of the Gaussian function. All the scales related to Hessian analysis can be

set from $\sqrt{2}/2$ to $2\sqrt{2}$ in order to match with various structure widths. In our experiments, the length for the structure element and the window size are all set to the same value for all the images. They do not need to be changed most of the time. A small range and value for the Gaussian scale σ_x is preferred because a large range will cause over-smoothing. Therefore the range for the Gaussian scale can also be regarded as a constant. The parameter which needs to be adjusted is the threshold ζ for V . We randomly picked four retinal images from the DRIVE database and tested the sensitivity of ζ . The result is shown in Fig. 17. From the graph, we can see that our method is not sensitive to parameter ζ . It shows that the MSE value will not change much when the threshold is set smaller than 2 or 0. So if there is no prior knowledge about the parameters, it is better to set the threshold to a small value.

Since the junction detection result will affect the final enhancement result, we also tested the robustness of the junction detection algorithm. We added different amount of Gaussian noise to the original images and showed two examples here (Fig. 18).

Then we calculated the mean precision and recall values based on the following equations:

$$\text{Precision} = \frac{tp}{tp+fp} \quad (10)$$

$$\text{Recall} = \frac{tp}{tp+fn} \quad (11)$$

$$\text{Accuracy} = (\text{Precision} + \text{Recall})/2 \quad (12)$$

Here tp represents true positives, fp represents false positives and fn represents false negatives. The values are listed in Table 2.

From Fig. 18, we can see, for the synthetic image, a good detection can still be obtained even noise is added. But when the complexity of the structure increases, the performance decreases. From the table, it shows the noise will disturb the performance of the junction detection algorithm, with an increase of precision value and decrease of recall as the noise increases. The reason is that the Gaussian profile of the linear structure may be affected by the noise but non-linear features still do not match with the template. We can still achieve 77.51% accuracy even noise with standard deviation 50 is added.

Our method takes about 70 s with a standard PC with an Intel Core i5 2.66 GHz processor and 4GB RAM to process a 403×328 pixel image shown in the second row in Fig. 13, while Frangi et al.'s method takes about 7 s and Shikata et al.'s method takes 4 s to process this image. Although the proposed method is more

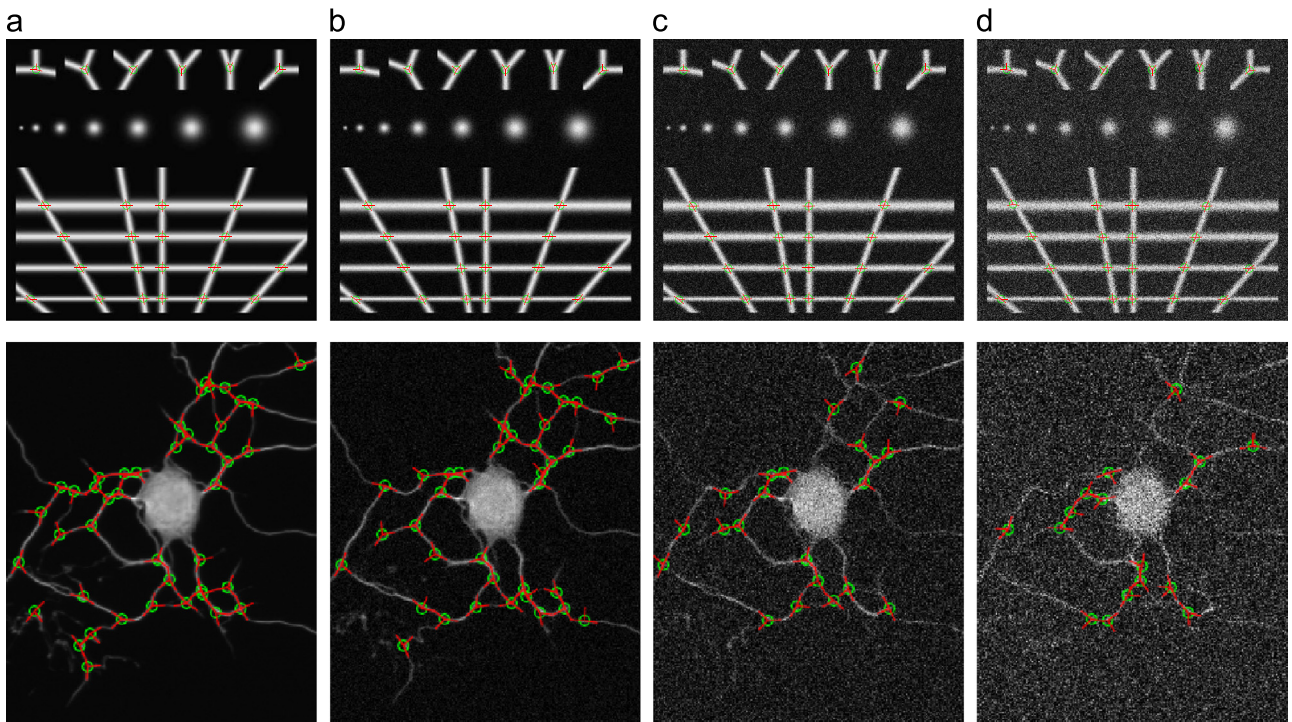


Fig. 18. The performance of the junction detection algorithm under different noise conditions. The red lines are the detected branches and the centre of the green circle represents the location of the junctions. (a) is the original input and the junction detection result, (b) shows the junction detection output when adding Gaussian noise (standard deviation=10) to the original image, (c) shows the junction detection output when adding Gaussian noise (standard deviation=30) and (d) shows the junction detection output when adding Gaussian noise (standard deviation=50). (For interpretation of the references to color in this figure caption, the reader is referred to the web version of this article.)

Table 2

Precision, recall and accuracy values when adding different Gaussian noise.

	Original input (%)	Gaussian noise 10 (%)	Gaussian noise 30 (%)	Gaussian noise 50 (%)
Precision	95.15	95.50	96.00	96.77
Recall	91.72	81.92	69.90	58.25
Accuracy	93.44	88.71	82.95	77.51

time-consuming, the better performance makes it more applicable in real applications.

7. Conclusions

In this paper, we propose a new method to enhance linear features and junctions in images. We enhance the linear features and junctions in two steps. In the linear structure enhancement, a multi-scale morpho-Gaussian filter is proposed to enhance the linear features. This method uses the enhancement function of the morphological operation and the smoothing function of the Gaussian filter. The use of multiple scales approach ensures that the linear structures with various widths can all be enhanced. Our morpho-Gaussian filter can give an enhanced as well as smoothed output. The broken linear parts can also be reconnected. Then we apply a multi-scale Hessian measurement to further enhance the linear features and reduce noise. We also develop a method for junction enhancement, which solves the problem of junction suppression with many existing methods. For junction enhancement, junctions are detected, decomposed and enhanced along each branch orientation. This step can solve the problem of junction suppression. Our tests on synthetic and real images show

very convincing results. We compare our method with Tankyevych et al.'s method, Kroon et al.'s method, Frangi et al.'s method and Shikata et al.'s method and give a quantitative analysis. The results show that the proposed method has a much better enhancement result in feature recovery, feature smoothing and noise removal and solve the junction suppression problem which exists in many other methods. The proposed method is significant that can be applied to the preprocessing for segmentation, centreline extraction and feature tracking. Our future work will focus on the implementation of the method on 3D images.

Conflict of Interest

None declared.

Acknowledgments

We would like to acknowledge and extend our gratitude to Xiao Tan at the University of New South Wales, Canberra, Australia, for his comments on this paper. We thank the anonymous reviewers for their helpful and constructive comments on this paper. The preliminary conference version of this paper was presented in [45].

References

- [1] M.J. Cree, D. Cornforth, H.F. Jelinek, Vessel segmentation and tracking using a two-dimensional model, in: Proceedings of Image and Vision Computing New Zealand, Dunedin, New Zealand, 2005, pp. 345–350.
- [2] Y. Kawata, N. Niki, T. Kumazaki, An approach for detecting blood vessel diseases from cone-beam CT image, in: Proceedings of the International

- Conference on Image Processing, vol. 2, Washington D.C., USA, 1995, pp. 500–503.
- [3] O. Chutatape, L. Zheng, S.M. Krishnan, Retinal blood vessel detection and tracking by matched Gaussian and Kalman filters, in: Proceedings of the 20th Annual International Conference of the IEEE Engineering in Medicine and Biology Society, vol. 20, Hong Kong, China, 1998, pp. 3144–3149.
 - [4] J. Lowell, A. Hunter, D. Steel, A. Basu, R. Ryder, R.L. Kennedy, Measurement of retinal vessel widths from fundus images based on 2-D modeling, *IEEE Trans. Med. Imaging* 24 (2004) 1196–1204.
 - [5] G.L. Wenk, Neuropathologic changes in Alzheimer's disease, *J. Clin. Psychiatr.* 64 (Suppl 9) (2003) 7–10.
 - [6] Z. Wang, A.C. Bovik, H.R. Sheikh, E.P. Simoncelli, Image quality assessment: from error visibility to structural similarity, *IEEE Trans. Image Process.* 13 (2004) 600–612.
 - [7] S. Chaudhuri, S. Chatterjee, N. Katz, M. Nelson, M. Goldbaum, Detection of blood-vessels in retinal images using two-dimensional matched-filters, *IEEE Trans. Med. Imaging* 8 (1989) 263–269.
 - [8] H. Li, W. Hsu, M.L. Lee, H. Wang, A piecewise Gaussian model for profiling and differentiating retinal vessels, in: Proceedings of 2003 International Conference on Image Processing, vol. 1, Barcelona, Catalonia, Spain, 2003, pp. 14–17.
 - [9] Y. Chen, L. Wang, L. Shi, D. Wang, P.-A. Heng, T.-T. Wong, X. Li, Structure-preserving multiscale vessel enhancing diffusion filter, in: Proceedings of IEEE 17th International Conference on Image Processing, Hong Kong, 2010, pp. 3565–3568.
 - [10] C. Lorenz, I.C. Carlsen, T.M. Buzug, C. Fassnacht, J. Weese, Multi-scale line segmentation with automatic estimation of width, contrast and tangential direction in 2D and 3D medical images, in: Proceedings of the 1st Joint Conference, Computer Vision, Virtual Reality and Robotics in Medicine and Medical Robotics and Computer-Assisted Surgery, Grenoble, France, 1997, pp. 233–242.
 - [11] Y. Sato, S. Nakajima, H. Atsumi, T. Koller, G. Gerig, S. Yoshida, R. Kikinis, 3D multi-scale line filter for segmentation and visualization of curvilinear structures in medical images, in: Proceedings of the 1st Joint Conference, Computer Vision, Virtual Reality and Robotics in Medicine and Medical Robotics and Computer-Assisted Surgery, Grenoble, France, 1997, pp. 213–222.
 - [12] A.F. Frangi, W.J. Niessen, K.L. Vincken, M.A. Viergever, Multiscale vessel enhancement filtering, in: Proceedings of the 1st International Conference on Medical Image Computing and Computer-Assisted Intervention, vol. 1496, Cambridge MA, USA, 1998, pp. 130–137.
 - [13] Q. Lin, Enhancement, extraction, and visualization of 3D volume data (Ph.D. thesis), Linkoping University, Linkoping, Sweden, 2003.
 - [14] P. Orłowski, M. Orkisz, Efficient computation of Hessian-based enhancement filters for tubular structures in 3D images, *IRBM* 30 (2009) 128–132.
 - [15] H. Shikata, E.A. Hoffman, M. Sonka, Automated segmentation of pulmonary vascular tree from 3D CT images, in: Proceedings of the SPIE International Symposium on Medical Imaging, vol. 5369, 2004, pp. 107–116.
 - [16] S.D. Olabarriaga, M. Breeuwer, W.J. Niessen, Evaluation of Hessian-based filters to enhance the axis of coronary arteries in CT images, in: Computer Assisted Radiology and Surgery: Proceedings of the 17th International Congress and Exhibition, vol. 1256, London, UK, 2003, pp. 1191–1196.
 - [17] P.T.H. Truc, M.A.U. Khan, Y.-K. Lee, S. Lee, T.-S. Kim, Vessel enhancement filter using directional filter bank, *Comput. Vis. Image Underst.* 113 (2009) 101–112.
 - [18] K. Deguchi, T. Izumitani, H. Hontani, Detection and enhancement of line structures in an image by anisotropic diffusion, *Pattern Recognit. Lett.* 23 (2002) 1399–1405.
 - [19] C. Cánero, P. Radeva, Vesselness enhancement diffusion, *Pattern Recognit. Lett.* 24 (2003) 3141–3151.
 - [20] K. Krissian, Flux-based anisotropic diffusion applied to enhancement of 3-D angiogram, *IEEE Trans. Med. Imaging* 21 (2002) 1440–1442.
 - [21] R. Manniesing, M.A. Viergever, W.J. Niessen, Vessel enhancing diffusion: a scale space representation of vessel structures, *Med. Image Anal.* 10 (2006) 815–825.
 - [22] D.-J. Kroon, C.H. Slump, T.J. Maal, Optimized anisotropic rotational invariant diffusion scheme on cone-beam CT, in: Proceedings of 13th International Conference on Medical Image Computing and Computer-Assisted Intervention, Beijing, 2010, pp. 221–228.
 - [23] M.H.F. Wilkinson, M.A. Westenberg, Shape preserving filament enhancement filtering, in: Proceedings of the 4th International Conference on Medical Image Computing and Computer-Assisted Intervention, vol. 2208, Utrecht, The Netherlands, 2001, pp. 770–777.
 - [24] O. Tankyevych, H. Talbot, P. Dokladal, Curvilinear morpho-Hessian filter, in: Proceedings of the 5th International Symposium on Biomedical Imaging, Paris, France, 2008, pp. 1011–1014.
 - [25] G. Agam, S.G. Armato III, C. Wu, Vessel tree reconstruction in thoracic CT scans with application to nodule detection, *IEEE Trans. Med. Imaging* 24 (2005) 486–499.
 - [26] M.S. Miri, A. Mahloojifar, Retinal image analysis using curvelet transform and multistructure elements morphology by reconstruction, *IEEE Trans. Biomed. Eng.* 58 (2011) 1183–1192.
 - [27] J. Oh, H. Hwang, Feature enhancement of medical images using morphology-based homomorphic filter and differential evolution algorithm, *Proc. Int. J. Control. Autom. Syst.* 8 (2010) 857–861.
 - [28] J. Song, E.J. Delp, A study of the generalized morphological filter, *Circuits Syst. Signal Process.* 11 (1992) 229–252.
 - [29] G. Matheron, *Random Sets and Integral Geometry*, Wiley, New York, USA, 1975.
 - [30] J. Serra, *Image Analysis and Mathematical Morphology*, Academic Press, New York, USA, 1982.
 - [31] P.A. Maragos, Morphological Filtering for Image Enhancement and Feature Detection. The Image and Video Processing Handbook, 2nd ed., Elsevier Academic Press, Burlington, MA, USA, 2005, pp. 135–156 (Chapter 3).
 - [32] T. Chanwimaluang, G. Fan, An efficient blood vessel detection algorithm for retinal images using local entropy thresholding, in: Proceedings of the 2003 International Symposium on Circuits and Systems, vol. 5, Bangkok, Thailand, 2003, pp. 21–24.
 - [33] M. Sofka, C.V. Stewart, Retinal vessel centerline extraction using multiscale matched filters, confidence and edge measures, *IEEE Trans. Med. Imaging* 25 (2006) 1531–1546.
 - [34] L. O'Gorman, An approach to fingerprint filter design, *Pattern Recognit.* 22 (1989) 29–38.
 - [35] B. Zhang, L. Zhang, L. Zhang, F. Karray, Retinal vessel extraction by matched filter with first-order derivative of Gaussian, *Comput. Biol. Med.* 40 (2010) 438–445.
 - [36] M. Sofka, C.V. Stewart, An improved matched filter for blood vessel detection of digital retinal images, *Comput. Biol. Med.* 37 (2007) 262–267.
 - [37] M. Cazorla, F. Escolano, D. Gallardo, R. Rizo, Junction detection and grouping with probabilistic edge models and Bayesian A*, *Pattern Recognit.* 35 (2002) 1869–1881.
 - [38] F. Deschênes, D. Ziou, Detection of line junctions and line terminations using curvilinear features, *Pattern Recognit. Lett.* 21 (2000) 637–649.
 - [39] T. Hansen, H. Neumann, A biologically motivated scheme for robust junction detection, in: Proceedings of the 2nd International Workshop on Biologically Motivated Computer Vision, vol. 2525, Tübingen, Germany, 2002, pp. 16–26.
 - [40] Y. Tao, Q. Gao, Vessel junction detection from retinal images, in: Proceedings of the 16th International Conference on Vision Interface, Halifax, Canada, 2003, pp. 388–394.
 - [41] R. Laganière, R. Elias, The detection of junction features in images, in: Proceedings of IEEE International Conference on Acoustics, Speech and Signal Processing, vol. 3, Montréal, Québec, Canada, 2004, pp. 573–576.
 - [42] D. Calvo, M. Ortega, M.G. Penedo, J. Rouco, Characterisation of feature points in eye fundus images, in: Proceedings of the 14th Iberoamerican Conference on Pattern Recognition: Progress in Pattern Recognition, Image Analysis, Computer Vision, and Applications, vol. 5856, Guadalajara, México, 2009, pp. 449–456.
 - [43] R. Su, C. Sun, T.D. Pham, Junction detection for linear structures based on Hessian correlation and shape information, *Pattern Recognit.* 45 (2012) 3695–3706.
 - [44] J. Staal, M.D. Abràmoff, M. Niemeijer, M.A. Viergever, B. van Ginneken, Ridge based vessel segmentation in color images of the retina, *IEEE Trans. Med. Imaging* 23 (2004) 501–509.
 - [45] R. Su, C. Sun, C. Zhang, T.D. Pham, Linear feature enhancement based on morphological operation and Gabor function, in: Proceedings of the 27th Image and Vision Computing New Zealand, Dunedin, New Zealand, 2012, pp. 91–96.

Ran Su obtained her PhD degree from the University of New South Wales, and spent her research co-training at CSIRO. Her main research interest is image analysis, pattern recognition and machine learning.

Changming Sun received the PhD degree in the area of computer vision from Imperial College London in 1992. Then, he joined CSIRO Computational Informatics, Australia, where he is currently a principal research scientist carrying out research and working on applied projects. His research interests include computer vision and photogrammetry, image analysis, and pattern recognition. He has served on the program/organizing committees of various international conferences. He is an Associate Editor for EURASIP Journal on Image and Video Processing, a SpringerOne journal. Dr. Sun is a member of the Australian Pattern Recognition Society.

Chao Zhang obtained his PhD degree from the University of New South Wales, and spent his research co-training at CSIRO. His main research interest is image analysis and pattern recognition.

Tuan D. Pham received his PhD in 1995 from the University of New South Wales (Sydney, Australia). His current research interests focus on image analysis and pattern recognition in medicine and biology. His research has been funded by government agencies, academic institutions, and industry. Dr. Pham is a senior member of the Institute of Electrical and Electronics Engineers (IEEE), editorial board member and associate editor of several journals and book series. He has served as chair and technical member of a number of international conferences, and the founder of the *International Symposium on Computational Models for Life Sciences* (CMLS) and The *International Aizu Conference on Biomedical Informatics and Technology* (ACBIT).